Experiments on Time Reversal Focusing of Acoustic Energy at a Crack Location in One Dimension

by

Brian Fehrman

Abstract

Place your abstract here

Nomenclature

$\vec{r}_0$	Location of source an emitting acoustic pulse
$\hat{\boldsymbol{R}}$	Reflection coefficient at $z = (L + l)$
$\hat{\boldsymbol{T}}$	Transmission coefficient at $z = (L = l)$
$\boldsymbol{R}$	Reflection coefficient at $z = l$
$\boldsymbol{T}$	Transmission coefficient at $z = l$
ϵ_{33}^{T}	PZT permittivity constant for the z direction
$\frac{\partial w_c}{\partial z}(l_c, t)$	Focused wave response at the crack location due to time reversal focusing
$\frac{\partial w_{cr}}{\partial z}$	Strain caused by wave portion transmitting to transducer B
$\frac{\partial w_{ct}}{\partial z}$	Strain caused by wave portion reflecting to transducer A
$\frac{\partial w}{\partial z}$	The strain resulting from the stress wave that is played by transducer A during the initial phase
∇^2	Laplacian operator

ν	Spatial dissipation factor
$\overline{R}$	Reflection coefficient at $z = l_c$
$\overline{T}$	Transmission coefficient at $z = l_c$
ρ^c	Density of the crack
ρ	Density of the transducer material
ρ^*	Density of the rod material
A	Cross-sectional area of the rod
a	Transducer cross sectional area
c^*	Velocity of wave propagation through the rod
C_{33}^*	Elastic constant in the z direction
C_{33}^c	Elastic coefficient of the crack in the z direction
C_c	Equivalent capacitance for the transducers
c_p	The speed of sound through the plate material.
C_{33}	PZT elastic constant in the z direction
D_3	Electric displacement in the z direction
d_{33}	Strain constant relating the strain and field intensity in the z direction

dz Differential element of length for the rod

E_3 Electric field intensity in the z direction

$h_i(\vec{r}_0)$ Integral of the transducer surface S_i

$h_i^{ac}(t)$ Function which relates pressure to voltage for the transducers

l Transducer length

l_T Distance from the crack to transducer B

P Axial pressure applied to rod end

S_{33} Strain in the z direction

T_3 Stress in the z direction

$V_a^+(i\omega)$ Reversed signal that is played back by Transducer A

$V_a^+(i\omega)$ Voltage produced by the wave at transducer A

$V_b^+(i\omega)$ Reversed signal that is played back by Transducer B

$V_b^+(i\omega)$ Voltage produced by the wave at transducer B

vec_r Position of the acoustic pressure field

w Displacement of the rod

Contents

List of Figures

Chapter 1

Introduction

Each day, more than 100 billion meteoroids larger than a micro-gram come speeding through Earth's atmosphere [1]. A large number of debris objects are presently in orbit around the earth (see Figure 1.1). NASA states that there are over 21,000 debris objects larger than a softball, 500,000 particles larger than a marble, and over 100 million smaller pieces that cannot be tracked. Due to the large number of objects traversing the space surrounding earth, it is likely that impact will occur with lightweight, low orbiting space structures and satellites which can result in varying degrees of damage [2]. The most likely impact will come from the smallest pieces as they occur in the largest numbers and are hard to avoid since they are hard to detect. These smaller particles will cause damage in the form of surface cracks and abrasions. Technologies exist such as the Whipple Shield (or meteor bumper) which help to mitigate the effects of impacts by absorbing some of the energy or breaking larger objects into smaller pieces [3]. However, it is still likely that particles can make it all the way to the underlying structure and cause damage which will build up over time. Access to these structures is difficult, costly, and dangerous. Repair missions will inevitably leave behind more debris which will increase the likelihood of future damage occurring to the structure being repaired as well as other structures in orbit. Materials with the ability to automatically heal damage as it occurs are very desirable for these applications [4].

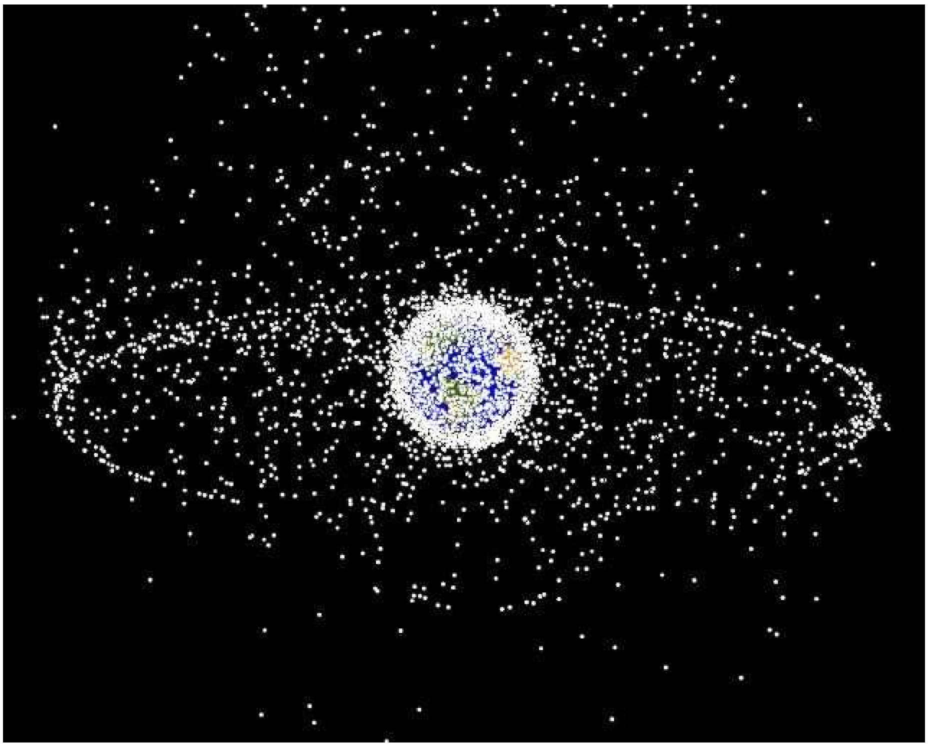

Figure 1.1: Image from NASA which depicts the debris objects that are currently orbiting the Earth. Some examples of debris objects include: broken spacecraft, upper stages of launch vehicles, debris that is intentionally released from missions, debris from collisions, and paint flecks. Much of the debris seems benign due to its size but is made dangerous by its high velocity (up to $60km/s/$s for smaller pieces). imagesource:[http://orbitaldebris.jsc.nasa.gov/photogallery/beehives/GEO640.jpg]

1.1 Self-Healing

Crack healing in materials owes some of its early studies to Wool and O'Connor who modeled crack healing in polymers and experimented with cantilever beams [5,6]. They found that polymer crack healing occurs in the following five stages: a) surface rearrangement, b) surface approach, c) wetting, d) diffusion, and e) randomization. Sloof, Song, and others have developed materials in which thermal activation caused a mending of cracks [7–11]. Caruso et. al. reported on material strength recovery in thermoplastics by using solvent-based healing agents [12]. Inspired by the idea of biological entities being able to automatically heal wounds, a self-healing material was made by White et. al. in which a catalyst and microcapsules filled with a reactive fluid were distributed throughout a material [13]. When the material was cracked, the capsules released their fluid which polymerized upon contacting the catalyst and effectively fused the faces of the crack together (Figure 1.2). Sottos et. al. have improved this self-healing implementation and found that damaged materials recovered up to 90% of their original strength [14]. The White and Sottos group have also studied crack healing by introducing hardener filled microcapsules into an epoxy that was molded into a double cantilever beam fracture specimen [15]. This concept has been extended to a self-healing coating that contained epoxy filled microcapsules and was tested on cold rolled steel sheets with good results [16]. Manuel et. al. created a matrix containing wires that could apply a force to the material to close a crack and then the material was heated to weld the crack together [17]. Adhesives with self-healing properties have been created by Jin et. al. and tested on composite laminates where they were found to increase the life of specimens subject to fatigue [18]. Self repairing chemicals have been successfully implemented on composite airplane components and were able to return to 88% of their original strength after impact and shear testing [19]. Recently, there has been a large interest in applying self-healing methods to help prolong the life of concrete which is very prone to cracks [20].

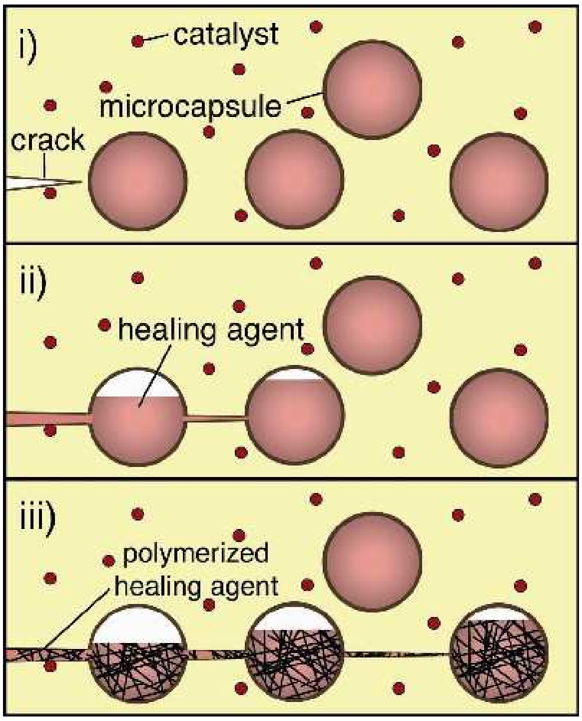

Figure 1.2: Concept drawing of a self-healing material in which micro-capsules filled with a reactive fluid and a catalyst are spread throughout that material. The drawing depicts the stages of damage, fluid release, and polymerization.
source:[http://www.howstuffworks.com/self-healing-spacecraft1.htm]

1.2 Accelerating the Self-Healing Process

Typically, the damaging process will continue to occur as the material attempts to mend itself together. It is therefore important that the material heals itself quickly so that the damage process does not dominate and prevent the material from reaching a full mechanical recovery. Studies have been performed on fatigue crack propagation in a self healing material [21]. Sheng, Burattini, and many others reported on increasing the healing rate by improving the materials that are used [22–26]. The use of U.V. light has been researched as a way to accelerate the healing process in metallopolymers and ethyl cellulose based copolymers [27,28]. Wool and O'Connor found in their work that an increase in pressure at the crack interface during the early stages of healing or an increase in temperature at any stage can increase the rate at which the material recovers [5]. Murphy et. al. have studied direct heating as a method to increase healing capabilities [29]. Direct heating to improve healing has also been applied to concrete [30, 31]. Applying pressure to a crack location via acoustic energy was studied by Korde et al. both theoretically and experimentally which found that acoustic energy can accelerate the healing process [32–34]. Fettig et. al. have also found that healing is optimized by ensuring good mixing in the early stages which can be brought about by localized pressure [35]. Sarrazin treated cracked nylon dog-bone specimens with ultrasonic probes which increased the temperature within the specimen and caused a fusing of the crack faces [36]. By using ultrasonic waves both the temperature and pressure at a recovery site could be increased which results in a faster healing time.

1.3 Implementation

Two main problems arise when implementing any of the previously described external stimulation methods to accelerate the healing process; i) detecting when damage has actually occurred and ii) applying the stimulation energy only to the damage location. In regards to i), it would be highly inefficient and potentially damaging to continually introduce energy if healing is not taking place. Along similar lines of reasoning, one would want only to apply energy to the actual recovery location for increased efficiency and so that unintended damage to the system does not occur. Acoustic energy is the method chosen here as it offers solutions to both problems.

1.3.1 Damage Sensing

Picture a rod with transducers on both ends that are capable of playing and recording sound. First, one transducer propagates a low energy acoustic stress-waves through the material and the other records the response of the material. If this process is repeated periodically and the response is monitored then a change in the response is observed if there is a change in the medium (e.g., damage has occurred; Figure 1.3). The acoustic energy could then be applied after this change in response has been detected and cease once the system determines that the response has returned to its initial state within some tolerance level. Imaging using ultrasonics has been around for some time now and is probably most recognized in ultrasounds that are used during pregnancy [37]. Ultrasonic imaging has been widely used in nondestructive testing to find cracks within structures. Harris et. al. used acoustic emission to monitor the fatigue crack growth in both aluminum and steel samples [38]. Detecting cracks in concrete by using ultrasound was reported by Zinin et. al. [39]. Acoustic waves have also been used to detect cracks in very fragile materials such as eggshells [40]. Recently, ultrasound has been used in dentistry to detect microcracks within teeth [41].

1.3.2 Time Reversal Focusing

Besides the mechanics of focusing the energy at the crack location, the problem arises that the location of the defect is not necessarily known. A method is needed that not only localizes the energy at the healing site but it does so without knowledge of the physical location of that site. Acoustic time reversal signal processing is one such method that possesses the aforementioned qualities. Picture again the cracked medium with transducers on both ends. As before, a stress-wave is played by one transducer. This time, however, both transducers record signals. The stress-wave propagates through the medium and strikes the crack which causes the wave to split into multiple components that transmit to the opposite transducer and reflect back to the original sending transducer where they are recorded. If the transducers re-

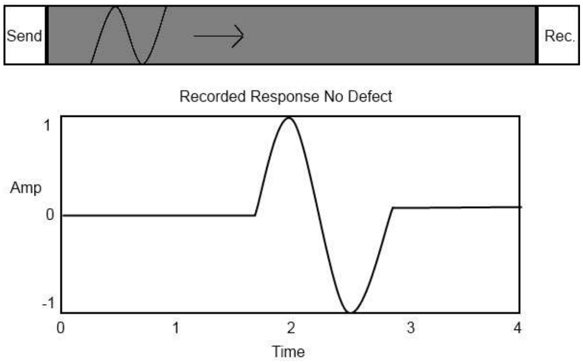

(a) Acoustic wave propagating through medium with no defect

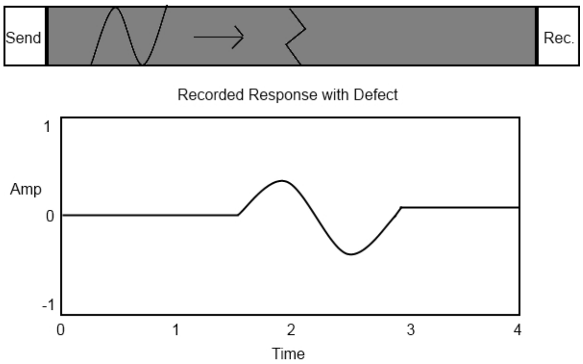

(b) Acoustic wave propagating through medium with a crack

Figure 1.3: a)A transducer sends an acoustic wave through a medium and a transducer on the opposite end records the response. This material is seen without a defect and the simulated response is shown; b) Same as a), but a defect is now present in the medium which causes a change in the response recorded on the opposite end and is seen in the simulated recorded response.

amplify and playback these signals in a time reversed fashion then the waves meet at the point where they split (here, the crack) which causes a focusing of their energy at that point. The focused wave splits again into multiple components that are recorded by each transducer and the time reversal process is repeated iteratively with a better focusing being achieved on each iteration until limits due to dissipation are reached (Figure 1.4 illustrates this concept). The time reversal concept can be extended to multiple dimensions in which the transducers are placed around the boundary. In a self-healing material, the focusing of energy at a crack location would accelerate the healing process at that site.

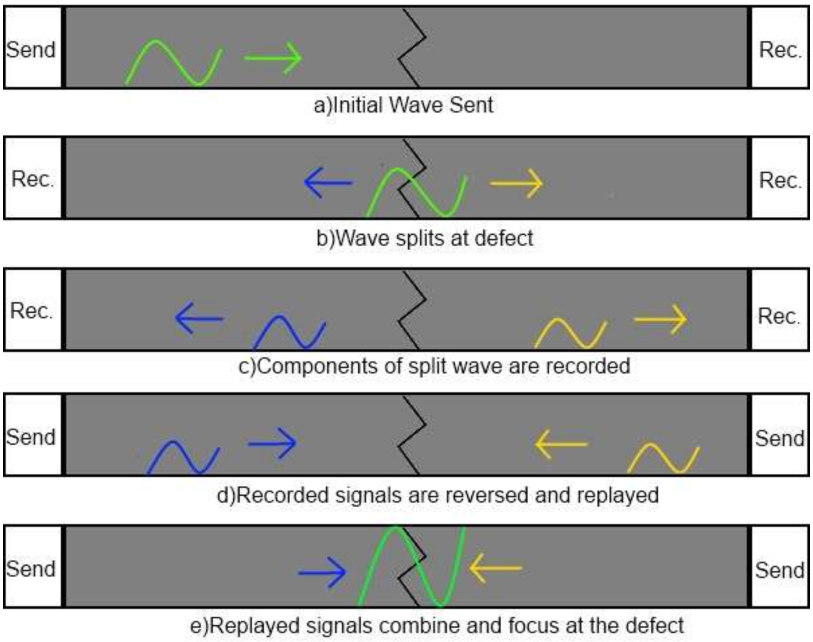

Figure 1.4: Concept drawing of time reversal in one dimension; a) An initial wave is sent out by a transducer; b) The wave travels down the rod until it hits the crack and splits into multiple components; c) The components of the incident wave travel towards each transducer where they are recorded; d) The recorded signals are amplified and replayed in a time reversed fashion; e) The wave components simultaneously reach the crack location where they first split and combine to cause a focusing of their amplitude at that point.

Mathematically, time reversal is the time domain analog of phase conjugation which has been used in adaptive optics to correct for wave front phase aberrations by forming a mirror to produce the conjugate phase aberrations of the incoming wave which results in a corrected wave front [42]. Acoustic time reversal has been studied extensively by Fink et. al. in which he first setup an array of transducers to send and receive ultrasonic waves through a rubber medium with random thicknesses and a hydrophone embedded as a reflector/receiver. Fink also has shown iterative focusing by experimenting with an array of transducers and two metal wires as reflectors. In the iterative experiments, it was shown that the energy focused on the strongest reflector after successive iterations [43]. Experiments were performed by Derode et. al. in which a transducer played a signal through a liquid containing over 2000 rods and an array of transducers located on the opposite side of the rods played the captured signals back and it was found that the replayed signals converged on the original source [44]. Time reversal has been applied to acoustic communications in both the ocean and air to achieve better signal to noise ratio by focusing the signal at the desired receiver [45–47]. Great promise has also been shown with applying time reversal to biomedical application such as the focusing of ultrasonic waves to destroy kidney stones or hyperthermia brain treatment [48]. The concept of time reversal is not only applicable to acoustics but can also be used with electromagnetic waves [49]. Liu et. al. have shown experimentally that bit-rate-errors in radio communications can be reduced by applying time reversal [50]. MIT has effectively created a microwave cannon by using the time reversal process to focus microwave energy [51].

1.4 Objectives

The overall goal, as devised by Dr. Korde, is to use time reversal acoustic focusing to accelerate the crack recovery process of a self-healing polymer by locally increasing the temperature and pressure. The work presented here looks at a subsection of that project which is the time reversal focusing at a crack location. There has been much theoretical and experimental work performed on applying time reversal in multiple dimensions. Here, the case of time reversal in one dimension is explored. Fouque et. al. performed calculations and simulations on one dimensional time reversal in random media with an embedded reflector to determine the reflector's location [52]. Korde performed calculations on focusing at a crack with piezoelectric transducers and time reversal processing [53]. To the author's knowledge, time reversal focusing at a defect location in one dimension has not been performed experimentally. In this work experiments are performed on circular steel and nylon rods with piezoelectric transducers to send and receive signals. This could have direct applications to the rods used in deployable space structures that may become cracked over time. Although the analysis is eased in this scenario, there are difficulties introduced in performing the experiments in one dimensional structures of finite length that are not present when performing time reversal in multiple dimensions. For instance, it is required that a transducer both sends a signal and reads a signal in the same iteration such that the ringing of the transducer may interfere with the signal being read.

The specific objectives of this work are to show:

1. Modeling and experimental verification of acoustic time reversal crack focusing in one dimension

2. Experimental verification of acoustic crack detection in one dimension

3. Experimental verification of iterative focusing and convergence of acoustic time reversal crack focusing in one dimension

    (a) Show that with each iteration, the amplitude seen at the defect increases until a convergence point is reached

Chapter 2

Modeling

This chapter begins with the models and derivations for the case of one dimensional time reversal and is based upon work performed by Korde [53]. Following that material will be a brief overview of two dimensional time reversal which is drawn from a number of published sources.

2.1 One Dimensional Wave Equation

In this section the one dimensional wave equation for a linear elastic material with uniform density and cross-sectional area will be derived. The derivation is based on knowledge from numerous books such as Kolsky [54] and Brown et. al. [55].

Figure 2.1 gives a basic diagram that is used for the wave equation derivation, with P being the axial pressure, dz being the material's differential element of length, and A being the cross-sectional area of the material. Define the stress in the z direction as:

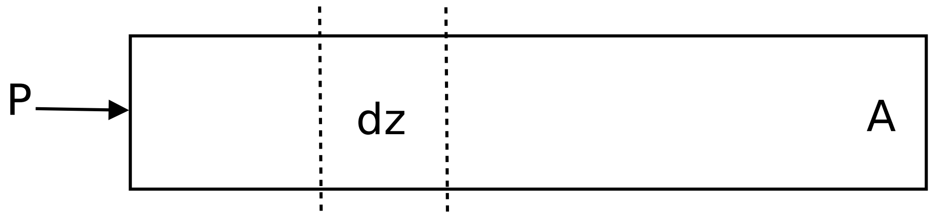

Figure 2.1: Diagram for deriving the one dimensional wave equation given an axial pressure applied to one end of the material with uniform density and cross-sectional area.

$$T_3 = \frac{P}{A} \tag{2.1}$$

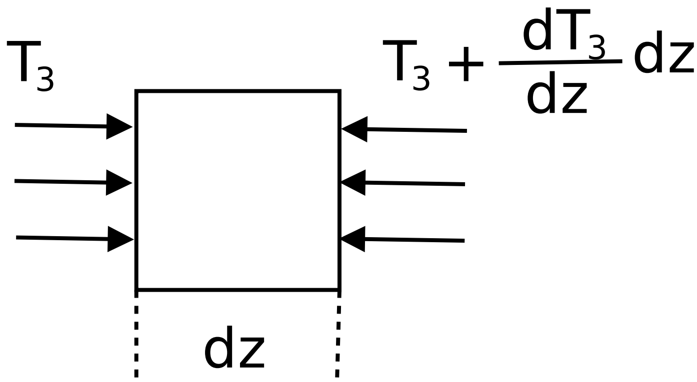

Figure 2.2: Differential element showing the stresses acting on the rod.

Applying Newton's second law and summing the forces,

$$-T_3 A + (T_3 + \frac{dT_3}{dz} dz)A = A\rho^* dz \frac{d^2 w}{dt^2} \tag{2.2}$$

With ρ^* being the density of the rod material and w being the displacement. Dividing through by the area,

$$-T_3 + T_3 + \frac{dT_3}{dz}dz = \rho^* dz \frac{d^2w}{dt^2} \tag{2.3}$$

$$\frac{dT_3}{dz}dz = \rho^* dz \frac{d^2w}{dt^2} \tag{2.4}$$

Canceling the dz term,

$$\frac{dT_3}{dz} = \rho^* \frac{d^2w}{dt^2} \tag{2.5}$$

C_{33}^* is the elastic constant in the z direction and is defined as the ratio of the stress and strain in the z direction. This is given by,

$$C_{33}^* = \frac{T_3}{S_{33}} \implies T_3 = C_{33}^* S_{33} \tag{2.6}$$

With S_{33} being the strain in the z direction. Strain is the ratio of the change in material length to the original length and in this case is given by,

$$S_{33} = \frac{dw}{dz} \tag{2.7}$$

Inserting 2.7 in to 2.6 we see that

$$T_3 = C_{33}^* \frac{dw}{dz} \tag{2.8}$$

Putting 2.8 back in to 2.5 and realizing that w is a function of both t and z,

$$C_{33}^* \frac{\partial^2 w}{\partial z^2} = \rho^* \frac{\partial^2 w}{\partial t^2} \tag{2.9}$$

Dividing through by ρ^* and moving the LHS term to the RHS, we arrive at

$$\frac{\partial^2 w}{\partial t^2} - c^{*2} \frac{\partial^2 w}{\partial z^2} = 0 \tag{2.10}$$

With c^* being the velocity of the wave propagation and is defined as,

$$c^* = \sqrt{\frac{C_{33}^*}{\rho^*}} \tag{2.11}$$

For the fixed-fixed unforced case, if we assume that $w(z,t)$ is a linear function then the solution can be found by a separation of variables approach. Let

$$w(z,t) = Z(z)T(t) \tag{2.12}$$

Inserting 2.12 into 2.10

$$\frac{\partial^2 ZT}{\partial t^2} - c^{*2} \frac{\partial^2 ZT}{\partial z^2} = 0 \tag{2.13}$$

Dividing through by ZT

$$\frac{1}{c^{*2}T} \frac{\partial^2 T}{\partial t^2} = \frac{1}{Z} \frac{\partial^2 Z}{\partial z^2} \tag{2.14}$$

Since Z and T are independent, this can only be true if each term is equal to some constant

$$\frac{1}{c^{*2}T}\frac{\partial^2 T}{\partial t^2} = \frac{1}{Z}\frac{\partial^2 Z}{\partial z^2} = -\lambda^2 \tag{2.15}$$

Then two ordinary differential equations are obtained

$$T''(t) + \lambda^2 c^{*2} T(t) = 0 \tag{2.16}$$

$$Z''(z) + \lambda^2 Z(z) = 0 \tag{2.17}$$

The solution for $Z(z)$ is

$$Z(z) = Acos(\lambda z) + Bsin(\lambda z) \tag{2.18}$$

Inserting the boundary conditions $Z(0) = 0$ and $Z(L) = 0$ 2.18 reduces to

$$Z(z) = B_n sin\left(\frac{n\pi z}{L}\right) \tag{2.19}$$

With

$$\lambda_n = \frac{n\pi}{L} \tag{2.20}$$

Now letting

$$\lambda_n c^{*2} = -\omega_n^2 \tag{2.21}$$

and inserting 2.21 in to 2.16 and applying a zero disturbance initial condition $\dot{T}(0) = 0$ the solution for $T(t)$ is found to be

$$T(t) = C_n cos(\omega_n t) \tag{2.22}$$

Combining 2.19 and 2.22 and summing to infinity the solution for $w(z,t)$ is found such that

$$w(z,t) = \sum_{n=1}^{\infty} A_n cos(\omega_n t) sin(\lambda_n z) \tag{2.23}$$

Applying the principles of orthogonality

$$A_n = \frac{2}{L} \int_0^L w(z,0) sin\left(\frac{\lambda_n z}{L}\right) dz \tag{2.24}$$

2.2 Piezoelectric transducers

This section describes the governing equations for d_{33} piezoelectric transducers that are placed on each end of a rod. The following work is based on derivations by Dr. Korde [53].

The constitutive equations for the transducers are:

$$T_3 = \overline{C_{33}} S_3 + \overline{d_{33}} D_3 \tag{2.25}$$

and

$$D_3 = \overline{\epsilon_{33}^T} E_3 + \frac{d_{33}}{s_{33}^E} S_3 \tag{2.26}$$

Where D_3, E_3, and d_{33} are the electric displacement, electric field intensity, and the strain constant relating strain and field intensity, respectively, all in the z direction. The other variables are given by the following equations:

$$s_{33}^E = \frac{1}{C_{33}} \tag{2.27}$$

$$\overline{C_{33}} = \frac{1}{s_{33}^E\left(1 - \frac{d_{33}^2}{s_{33}^E \epsilon_{33}^T}\right)} \tag{2.28}$$

$$\overline{d_{33}} = -\frac{d_{33}/\epsilon_{33}^T}{s_{33}^E\left(1 - \frac{d_{33}^2}{s_{33}^E \epsilon_{33}^T}\right)} \tag{2.29}$$

$$\overline{\epsilon_{33}^T} = -\frac{\epsilon_{33}^T}{s_{33}^E\left(1 - \frac{d_{33}^2}{s_{33}^E \epsilon_{33}^T}\right)} \tag{2.30}$$

With C_{33} and ϵ_{33}^T being the PZT elastic constant in the z direction and permittivity constant in the z direction respectively.

The equivalent circuits for the transducers are modeled as a resistor and capacitor in series as shown in Figure 2.3 and with C_c being the equivalent capacitance and is given by

$$C_c = \overline{\epsilon_{33}} \pi a^2 / l \tag{2.31}$$

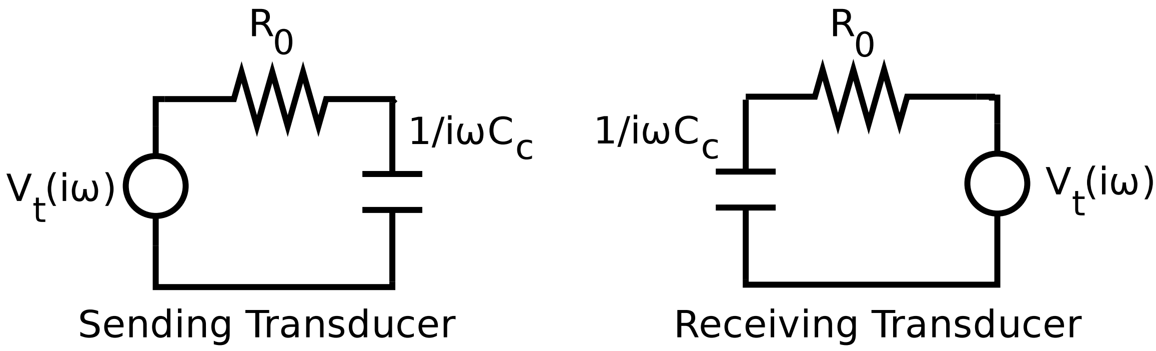

Figure 2.3: Equivalent circuit diagram for the piezoelectric transducers.

Where a and l are the transducer area and length respectively.

2.3 Rod with Transducers

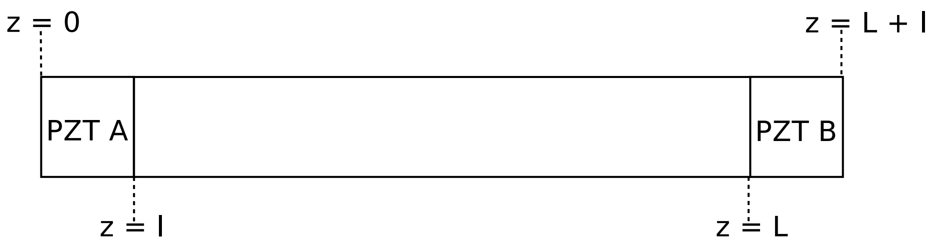

Figure 2.4: Diagram of a rod with d_{33} piezoelectric transducers placed on each end.

Consider a rod with d_{33} transducers affixed to each end as pictured in Figure 2.4. We wish to model propagation of a wave through the system with the wave being sent by one of the transducers. The one-dimensional wave results from Section 2.1 can be applied here such that the equation of the motion for the wave propagating through the transducers is the same as through the rod but with a different density and elastic coefficient which will be denoted as ρ and C_{33} respectively. The wave velocity through the transducer is then described as

$$c = \sqrt{\frac{C_{33}}{\rho}} \tag{2.32}$$

So for $0 \leq z \leq l$ and $L < z \leq (L + l)$ we have

$$\frac{\partial^2 w}{\partial t^2} - c^2 \frac{\partial^2 w}{\partial z^2} = 0 \tag{2.33}$$

For the rod domain, $l < z \leq L$, we just apply equation 2.10. Let the stress and deflection across the interfaces be continuous. When a wave encounters either of the interfaces it will experience refraction in which part of the wave will be reflected and part will be transmitted into the next medium. This phenomena can be accounted for by finding the reflection and transmission coefficients for each interface. For $z = l$ these coefficients are found to be

$$\boldsymbol{R} = \frac{\overline{C_{33}} + \frac{\overline{d_{33}} d_{33}}{2 s_{33}^E} - C_{33}^*}{\overline{C_{33}} + \frac{\overline{d_{33}} d_{33}}{2 s_{33}^E} + C_{33}^*} \tag{2.34}$$

$$\boldsymbol{T} = \frac{2\left(\overline{C_{33}} + \frac{\overline{d_{33}} d_{33}}{2 s_{33}^E}\right)}{\overline{C_{33}} + \frac{\overline{d_{33}} d_{33}}{2 s_{33}^E} + C_{33}^*} \tag{2.35}$$

Similarly, for the interface at $z = (L + l)$

$$\hat{\boldsymbol{R}} = \frac{\overline{C_{33}} - \frac{\overline{d_{33}} d_{33}}{2 s_{33}^E} - C_{33}^*}{\overline{C_{33}} + \frac{\overline{d_{33}} d_{33}}{2 s_{33}^E} + C_{33}^*} \tag{2.36}$$

$$\hat{\boldsymbol{T}} = \frac{2C^*_{33}}{\overline{C_{33}} + \frac{\overline{d_{33}}d_{33}}{2s^E_{33}} + C^*_{33}} \tag{2.37}$$

2.4 Cracked Rod with Transducers

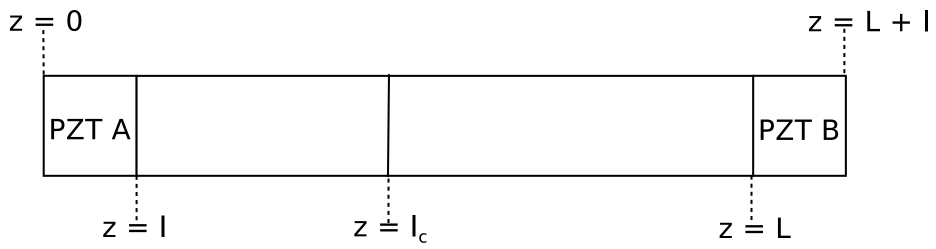

Figure 2.5: Diagram of a rod with d_{33} piezoelectric transducers placed on each end and a crack located at an arbitrary location within the system, with l_c being the distance of the crack from the origin and is not known a prior.

In this section a crack located at an arbitrary position is introduced into the system modeled in Section 2.3 and is shown in Figure 2.5. The crack can be modeled as another interface boundary within the system as we saw previously. If a stress wave is played out from one of these transducers, say transducer A, then it will travel through the rod and refracts upon reaching the crack location due to a change in the medium. The crack can then be accounted for as a change in the material density and elastic coefficient from ρ^* to ρ^c and from C^*_{33} to C^c_{33} respectively. Again, let the stress and strain at the crack interface be continuous. As seen before we will have a reflection coefficient and a transmission coefficient which are given by

$$\overline{\boldsymbol{R}} = \frac{C^*_{33} - C^c_{33}}{C^*_{33} + C^c_{33}} \tag{2.38}$$

$$\overline{\boldsymbol{T}} = \frac{2C_{33}^{*}}{C_{33}^{*} + C_{33}^{c}} \tag{2.39}$$

2.5 One Dimensional Time Reversal Focusing at a Crack

Considered here is the time reversal playback of the system modeled thus far. First there is an interrogatory phase in which transducer A plays out a stress wave which will propagate along the rod towards transducer B on the opposite end. When the wave reaches the crack location it will refract causing part of its energy to be transmitted and part to be reflected and is described by the coefficients shown in Section 2.4. The strain caused by the wave reflected portion returning to the transducer A is

$$\frac{\partial w_{cr}}{\partial z} = \overline{\boldsymbol{R}}\frac{\partial w_t}{\partial z} \tag{2.40}$$

For the transmitted portion of the wave, its strain will be

$$\frac{\partial w_{ct}}{\partial z} = \overline{\boldsymbol{T}}\frac{\partial w_t}{\partial z} \tag{2.41}$$

In both 2.40 and 2.41

$$\frac{\partial w_t}{\partial z} = \boldsymbol{T}\frac{\partial w}{\partial z} \tag{2.42}$$

This will create a voltage at transducer A which is found in the frequency domain as

$$V_a^+(i\omega) = -\frac{d_{33}\pi a^2}{2s_{33}^E C_c}\frac{\partial w_{cr}}{\partial z}(i\omega) \tag{2.43}$$

and at transducer B

$$V_b^+(i\omega) = \frac{d_{33}\pi a^2}{2s_{33}^E C_c}\hat{\boldsymbol{T}}\frac{\partial w_{ct}}{\partial z}(i\omega) \tag{2.44}$$

These voltages are recorded by each of the transducers. The reversal of these recorded voltages is just the complex conjugate for each signal such that the replayed voltage by each transducer will be

$$V_a^+R(i\omega) = V_a^+ * (i\omega) \tag{2.45}$$

and

$$V_b^+R(i\omega) = V_b^+ * (i\omega) \tag{2.46}$$

In addition to playing back the reversed signals, each transducer must also play back an idle period to account for the wave propagation time and the likely possibility that the crack is located closer to one transducer than the other. This information is inferred from the signal recorded and the appropriate zero period is added to the transducers. If the reversed signals are played back by each transducer with the necessary idle periods then the waves reach the defect at the same instant where they constructively interfere. The combined strain produced at the defect in the time domain form is found to be

$$\frac{\partial w_c}{\partial z}(l_c, t) = -\frac{2s_{33}^E \boldsymbol{T}}{d_{33}\pi a^2 R_0} V_0 \delta(t) \left(\frac{\hat{\boldsymbol{T}} M \boldsymbol{T}}{R_0 C_c}\right) \times \\ \left(\overline{\boldsymbol{R}}(-2\nu l_c) + \overline{\boldsymbol{T}} \exp(-2\nu l_T) \times \exp\left[-\frac{1}{R_0 C_c}\left(t - \frac{3l_c}{c^*} - \frac{2l}{c}\right)\right]\right) \tag{2.47}$$

Where ν is a spatial dissipation factor and l_T is the distance from the crack to transducer B.

Through the use of Green functions it is found that the amplification of the focusing at the defect will increase if the time reversal is applied in an iterative fashion such that after each transducer replays a time reversed signal it records the new response and plays that record back in a time reversed fashion. This amplification will continue until it becomes limited by material dissipation at which point the algorithm has converged. Because the rod is of finite length there will be natural vibrations produced when the rod is excited. However, it is argued that if a sufficient delay time is introduced between successive iterations then natural vibrations of the rod die down while the amplification at the crack location increases.

2.6 Time Reversal Focusing in Two Dimensions

Here a brief overview is given of focusing acoustic energy in two dimensions using the time reversal method and is drawn from Fink [56]. Figure 2.6 depicts a scenario in

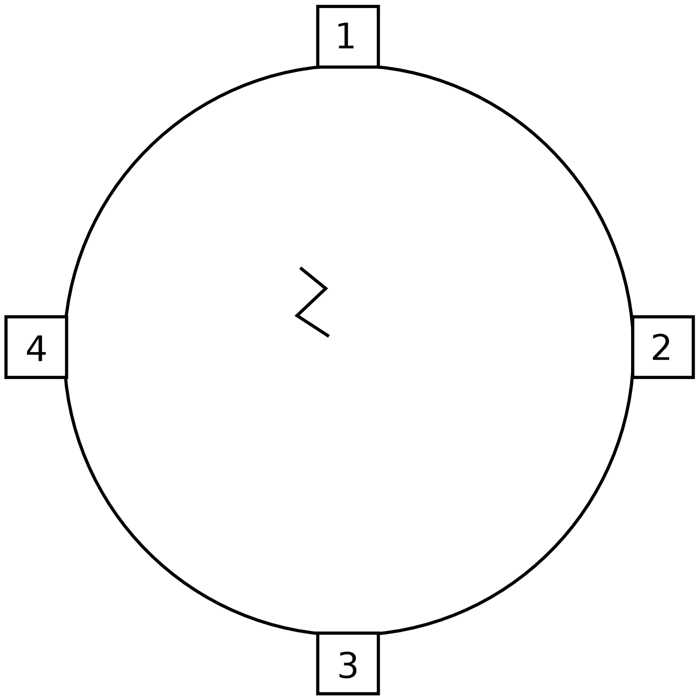

Figure 2.6: Concept diagram of a two dimensional time reversal setup in which transducers are located around the boundary of a circular plate. A crack exists on the plate and is the point at which the transducers will focus acoustic energy.

which transducers are located around the boundary of a plate and a defect is located at an arbitrary position on the plate. The method used to focus acoustic energy at the crack is a natural extension of the time reversal method used for the rod. The equation of motion for the wave propagation is the similar to 2.10 except we now introduce the Laplacian to account for the multiple spatial dimensions which gives

$$\frac{\partial^2 w}{\partial t^2} - c_p^2 \nabla^2 w(\vec{r}, t) = 0 \tag{2.48}$$

Where c_p is the speed of sound through the plate material and $\vec{r}$ is the position of the acoustic pressure field.

As before, a transducer sends out an initial pulse. Let the field produced in $\vec{r}$ at time t caused by a pulse emitted at time t_0 by a source located at $\vec{r}_0$ be represented by a Green function

$$G(\vec{r}_0, t_0|\vec{r}, t) \tag{2.49}$$

Because of the reciprocity theorem,

$$G(\vec{r}_0, t_0|\vec{r}, t) = G(\vec{r}, t_0|\vec{r}_0, t) \tag{2.50}$$

Which means that if $\vec{r}$ replays the pulse it feels due to $\vec{r}_0$ then $\vec{r}_0$ will experience that same excitation. Let the integral over the transducer surface S_i be

$$h_i(\vec{r}_0) = \int_{S_i} G(\vec{r}_0, t_0|\vec{r}, t)dr = \int_{S_i} G(\vec{r}, t_0|\vec{r}_0, t)dr \tag{2.51}$$

The function relating pressure to voltage for the transducers is written as

$$h_i^{ac}(t) \tag{2.52}$$

After the wave sent by a transducer reaches the defect in the plate, it will refract and the crack will act as an acoustic source located at $\vec{r}_0$. The voltage recorded by each transducer is seen as the convolution of

$$h_i^{ac}(t) * h_i(\vec{r}_0, t) \tag{2.53}$$

These signals are time reversed for each transducer such that the replayed signals are

$$h_i^{ac}(T-t) * h_i(\vec{r}_0, T-t) \tag{2.54}$$

The response at the crack due to one transducer is the convolution of the replayed signal and the original pulse emitted from the crack

$$h_i^{ac}(T-t) * h_i(\vec{r}_0, T-t) * h_i(\vec{r}_0, t) * h_i^{ac}(t) \tag{2.55}$$

The contribution due to all of the transducer is simply the sum over i of the individual contributions

$$\sum_i h_i^{ac}(T-t) * h_i(\vec{r}_0, T-t) * h_i(\vec{r}_0, t) * h_i^{ac}(t) \tag{2.56}$$

Chapter 3

Experiments

Chapter 4

Results

Chapter 5

Recommended Future Work

Chapter 6

Conclusion

Bibliography

[1] Sigrid Close. Shooting Stars Can Shoot Down Satellites. http://spectrum.ieee.org/aerospace/satellites/shooting-stars-can-shoot-down-satellites/2, April 2010. [Online; accessed 15-August-2012].

[2] NASA. Orbital Debris. http://www.nasa.gov/mission_pages/station/news/orbital_debris.htm March 2012. [Online; accessed 15-August-2012].

[3] NASA. Hypervelocity Impact Technology. http://ares.jsc.nasa.gov/ares/hvit/index.cfml, August 2012. [Online; accessed 16-August-2012].

[4] B.L. Lee. Multifunctional design perspective for self-healing and autonomic response. Final Program and Abstract Book 2nd ICSHM - 28 June - 1 July 2009.

[5] R.P. Wool and K.M. O'Connor. A Theory of Crack Healing in Polymers. *J. Applied Physics*, 52(10):5953–5963, October 1981.

[6] R.P. Wool and K.M. O'Connor. Time dependence of crack healing. *J. Polymer Science*, 20(1):7–16, January 1982.

[7] G. M. Song, Y. T. Pei, W. G. Sloof, S. B. Li, S. van der Zwaag, and J. Th. M. De Hosson. Oxidation-induced crack healing in Ti_3AlC_2 ceramics. Final Program and Abstract Book 2nd ICSHM - 28 June - 1 July 2009.

[8] W. G. Sloof. Self-healing mechanism in material for high temperature applications. Final Program and Abstract Book 2nd ICSHM - 28 June - 1 July 2009.

[9] A. W. Bosman. Supramolecular materials in motion. Final Program and Abstract Book 2nd ICSHM - 28 June - 1 July 2009.

[10] R. Djugum and R. N. Lumley. Healing and crack closure in an Al-Cu alloy by remedial heat treatment. Final Program and Abstract Book 2nd ICSHM - 28 June - 1 July 2009.

[11] X. Luo, R. Ou, D. E. Eberly, A. Singhal, W. Viratyaporn, and P. T. Mather. A thermoset/thermoplastic blend based thermally mendable, self-healing material. Final Program and Abstract Book 2nd ICSHM - 28 June - 1 July 2009.

[12] M. M. Caruso, C. L. Mangun, E. D. Wetzal, J. A. Orlicki, N. R. Sottos, S. R. White, and J. S. Moore. Self-healing of thermoplatic materials using solvent-based healing agents. Final Program and Abstract Book 2nd ICSHM - 28 June - 1 July 2009.

[13] S.R. White, N.R. Sottos, P.H. Guebelle, J.S. Moore, M. R. Kessler, S.R. Sriram, E.N. Brown, and S. Viswanathan. Autonomic healing of polymer composites. *Letters to Nature*, 409(15):794–817, February 2001.

[14] N.R. Sottos. Recent advances in microcapsule and microvascular based self-healing polymers. In *2nd Int. Conf. on Self-Healing Materials*, 2009. Chicago, IL; 28 June – 1 July 2009.

[15] D. A. Mcllroy, B. J. Blaiszik, N. R. Sottos, and S. R. White. Analysis of a two-part self-healing system with encapsulated hardening agent. Final Program and Abstract Book 2nd ICSHM - 28 June - 1 July 2009.

[16] Yang Zhao, Wei Zhang, Le ping Liao, Si jie Wang, and Wu jun Li. Self-healing coatings containing microcapsule. *Applied Surface Science*, 258(6), 2012.

[17] M.V. Manuel and G.B. Olson. Analysis of a two-part self-healing system with encapsulated hardening agent. Final Program and Abstract Book 2nd ICSHM - 28 June - 1 July 2009.

[18] H. Jin, G. Miller, N. R. Sottos, and S. R. White. Self-healing adhesives. Final Program and Abstract Book 2nd ICSHM - 28 June - 1 July 2009.

[19] C. Dry. Self repair of composites for airplane components. Final Program and Abstract Book 2nd ICSHM - 28 June - 1 July 2009.

[20] Min Wu, Bjorn Johannesson, and Mette Geiker. A review: Self-healing in cemetitious materials and engineered cementitious composite as a self-healing material. *Construction and Building Materials*, 28(1), 2012.

[21] E.N. Brown, S.R. White, N.R. Sottos, and P.H. Guebelle. Fatigue Crack Propagation in a Self-Healing Polymer Composite. SEM Annual Conference 2003, 2003.

[22] X. Sheng, T. C. Mauldin, and M. R. Kessler. Design and synthesis of next-generation monomer healing agents. Final Program and Abstract Book 2nd ICSHM - 28 June - 1 July 2009.

[23] S. Burattini, B. W. Greenland, H. M. Colquhoun, and W. Hayes. A rapidly healable supramolecular polymeric blend. Final Program and Abstract Book 2nd ICSHM - 28 June - 1 July 2009.

[24] W. Nakao and S. Abe. Self-healing rate improvement by shape modification of dispersed silicon carbide particles. Final Program and Abstract Book 2nd ICSHM - 28 June - 1 July 2009.

[25] V. A. Imperiale and I. P. Bond. A novel self-healing agent able to improve the residual strength of cfrp after impact. Final Program and Abstract Book 2nd ICSHM - 28 June - 1 July 2009.

[26] Chun-Sheng Zhang and Qing-Qing Ni. Bending behavior of shape memory polymer based laminates. *Science Direct - Composite Structures*, 78:153–161, 2007.

[27] X. Tang, X. Liang, X. Fan, and Q. Zhou. Syntehsis of ethyl cellulose-based thermal- and photo- dual responsive copolymers via atrp and their aggregates in solution. Final Program and Abstract Book 2nd ICSHM - 28 June - 1 July 2009.

[28] M. Burnworth, S. J. Rowan, and C. Weder. Optically responsive metallopolymers. In *2nd Int. Conf. on Self-Healing Materials*, 2009. Chicago, IL; 28 June – 1 July 2009.

[29] E. B. Murphy, M. L. Auad, and F. Wudl. Stimuli-responsive healable materials: Diels-alder based mending. Final Program and Abstract Book 2nd ICSHM - 28 June - 1 July 2009.

[30] A. Garcia, E. Schlangen, and M. van de Ven. Closing cracks on conductive asphalt mortar by induction heating. Final Program and Abstract Book 2nd ICSHM - 28 June - 1 July 2009.

[31] T. Nishiwaki, H. Mihasi, Y. Okuhara, and H. Terashima. Development of self-repairing concrete system using selective heating devices. Final Program and Abstract Book 2nd ICSHM - 28 June - 1 July 2009.

[32] J.C. Sarrazin, C.H. Jenkins, U.A. Korde, and S.A. Rutherford. Ultrasonic self-

healing of polymers. In *2nd Int. Conf. on Self-Healing Materials*, 2009. Chicago, IL; 28 June – 1 July 2009.

[33] A.J. Cushman, B.C. Fehrman, U.A. Korde, and S.D. Gruenig. Experiments on the focusing and use of acoustic energy to accelerate polymer healing. In *SPIE 2012 SDM Conference*, 2012. San Diego, CA; 12 March - 16 March 2012.

[34] K.A. Barnes, U.A. Korde, C.H. Jenkins, and R.M. Winter. On the use of acoustic excitation to accelerate self healing in polymers. In *2nd Int. Conf. on Self-Healing Materials*, 2009. Chicago, IL; 28 June – 1 July 2009.

[35] J. W. Fettig and J. B. Freund. Multi-phase simulation of microvascular self-healing materials. Final Program and Abstract Book 2nd ICSHM - 28 June - 1 July 2009.

[36] J.C. Sarrazin. Ultrasonic repair of polymers: Fundamentals and modeling for self-healing. Master's thesis, Montana State University, 2009.

[37] obyn.net. The History of Ultrasound: A collection of recollections, articles, interviews, and images. www.obgyn.net, 2006. [Online; accessed 22-August-2012].

[38] D. O. Harris and H.L. Dunegan. Continuous monitoring of fatigue-crack growth by acoustic-emission techniques. *Experimental Mechanics*, 14(2):s71–s81, 1974.

[39] P. Zinin, M. H. Manghnani, Y. C. Wand, and R. A. Livingston. Detection of

cracks in concrete composites using acoustic microscopy. *NDT & E International*, 33(5), 2000.

[40] B. De Ketelaere, P. Coucke, and J. De Baerdemaker. Eggshell Crack Detection based on Acoustic Resonance Frequency Analysis. *Journal of Agricultural Engineering Research*, 76(2), 2000.

[41] M. Matsushita-Tokugawa, Jiro Miura, and Takahide Sakagami. Detection of Dentinal Microcracks Using Infrared Thermography. *Journal of Endodontics*, 2012.

[42] D.M. Pepper. Nonlinear optical phase conjugation. *Optical Engineering*, 21:156–183, 1982.

[43] M. Fink. Time-reversal mirrors. *J. Phys. D: Appl. Phys*, 26, March 1993.

[44] Arnaud Derode, Philippe Roux, and Mathias Fink. Robust acoustic time reversal with high-order multiple scattering. *Phys. Rev. Lett*, 75, May 1995.

[45] Kevin Smith, Antonio Abrantes, and Andres Larraza. Examination of time-reversal acoustics in shallow water and applications to noncoherent underwater communications. *J. Acoustical Society of America*, 113(6), 2003.

[46] Aijun Song and Moshen Badiey. Time reversal acoustic communication for multi-band transmission. *J. Acoustical Society of America*, 132(4), 2012.

[47] T. Shimura, Y. Watanabe, H. Ochi, and H. C. Song. Long-range time reversal communication in deep water: Experimental results. *J. Acoustical Society of America*, 132(1), 2012.

[48] M. Fink, G. Montaldo, and M. Tanter. Time-reversal acoustics in biomedical engineering. *Annual Review of Biomedical Engineering*, 5, June 2003.

[49] G. Lerosey, J. de Rosny, A. Tourin, A. Derode, G. Montaldo, and M. Fink. Time-reversal of electromagnetic waves. *Phys. Revised Letters*, 92, 2004.

[50] X.-F. Liu, B.-Z. Wang, S.-Q. Xiao, and J. H. Deng. Performance of impulse radio uwb communications based on time reversal technique. *Progress In Electromagnetics Research*, 79, 2008.

[51] Matthieu Davy, Julien de Rosny, Jean-Chrisophe Joly, and Mathias Fink. Focusing and amplification of electromagnetic waves by time reversal in an leaky reverberation chamber. *Propagation and Remote Sensing*, 11, January 2010.

[52] J-P Fouque and O.V. Poliannikov. Time reversal detection in one-dimensional random media. *Institute of Physics Publishing*, 22, June 2006.

[53] B. C. Fehrman and U. A. Korde. Targeted delivery of acoustic energy for self-healing. Submitted for review to Journal of Intelligent Material Systems and Structures, 2012.

[54] H. Kolsky. *Stress Waves in Solids*. Dover Publications, 1963.

[55] James Ward Brown and Ruel V. Churchill. *Fourier Series and Boundary Value Problems*. Tata McGraw-Hill, 7th edition, 2008.

[56] M. Fink. Time-reversal of ultrasonic fields–part i: Basic principles. *IEEE Transactions on Ultrasonics, Ferrorelectrics, and Frequency Control*, 39(5), September 1992.